ACS OMEGA

http://pubs.acs.org/journal/acsodf

Article

Isocoumarins and Benzoquinones with Their Proprotein Convertase Subtilisin/Kexin Type 9 Expression Inhibitory Activities from Dried Roots of *Lysimachia vulgaris*

Pisey Pel, Young-Mi Kim, Hyun Ji Kim, Piseth Nhoek, Chae-Yeong An, Min-Gyung Son, Hongic Won, Seung Eun Lee, Jeonghoon Lee, Hyun Woo Kim, Young Hee Choi, Chang Hoon Lee, and Young-Won Chin*

Cite This: *ACS Omega* 2022, 7, 47296−47305

Read Online

ACCESS | Metrics & More | Article Recommendations | Supporting Information

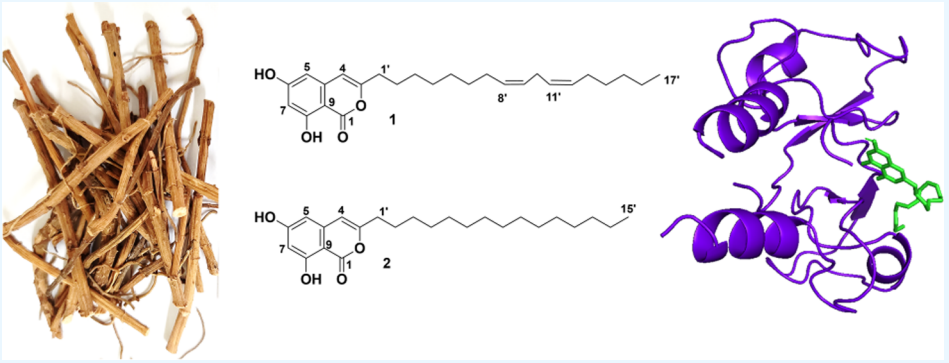

ABSTRACT: A phytochemical investigation of the *n*-hexane-soluble chemical constituents *of Lysimachia vulgaris* roots allowed for selection using a proprotein convertase subtilisin-kexin type 9 (PCSK9) mRNA expression monitoring assay in HepG2 cells. This led to the isolation of two previously undescribed isocoumarins of natural origin, 8′*Z*,11′*Z*-octadecadienyl-6,8-dihydroxyisocoumarin (**1**) and 3-pentadecyl-6,8-dihydroxyisocoumarin (**2**), along with 20 previously reported compounds (**3**−**22**). All of the structures were established using NMR spectroscopic data and MS analysis. Of the isolates, **1** and **3** were found to inhibit PCSK9, inducible degrader of the low-density lipoprotein receptor (IDOL), and SREBP2 mRNA expression. Further computational dockings of both **1** and **3** to C-ring of IDOL E3 ubiquitin ligase predicted the mechanism behind the inhibitory effect of these compounds on the enzyme.

1. INTRODUCTION

Lysimachia vulgaris L., also known as yellow loosestrife, grows naturally worldwide and is often used as a commercial garden plant.[1] In Asia,[2,3] Europe,[1,4] and North America,[3] the flowers and young leaves of *L. vulgaris* are consumed as tea and vegetables. In particular, it is registered as a food ingredient in the Korean Food Standards Codex.[2,3] Moreover, *L. vulgaris* leaves have been used in folk medicine to treat diarrhea,[1,3,4] dysentery, fever, bleeding, and wounds.[1,4] Previous studies on this plant have reported the following chemical constituents: benzoquinones,[1,4] flavonoids,[1,2,4] phenolic acids,[2] saponins,[1,4] and tannins.[1,4] Additionally, pharmacological investigations on *L. vulgaris* extracts have demonstrated their analgesic,[5] antibacterial,[3,4] antioxidant,[2,3] antipyretic,[1] antitumor,[2,4] and cytotoxic properties.[4]

Despite the efficacy of statins in lowering low-density lipoprotein cholesterol (LDLC) levels and decreasing cardiovascular disease risk,[5−8] there are also challenges related to both their insufficient therapeutic effects and side effects in patients with familial hypercholesterolemia.[7,8] The LDL receptor (LDLR) plays a prominent role in lowering the LDLC level of the blood by trafficking LDLC from the blood into cells.[5−9] Two major regulator proteins of LDLRs, proprotein convertase subtilisin/kexin type 9 (PCSK9) and inducible degrader of the low-density lipoprotein receptor (IDOL), are known to regulate LDLR degradation.[7−11] PCSK9 binds to the extracellular domain of LDLRs on the cell membrane, promoting the degradation and preventing the recycling of LDLR. This leads to a low level of LDLR in the cell membrane and less uptake of LDLC into the cell. Hence,

Received: October 16, 2022
Accepted: November 28, 2022
Published: December 8, 2022

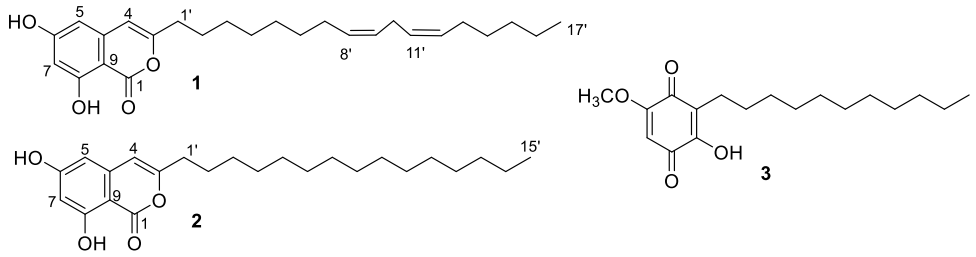

Figure 1. Representative new and active compounds **1**−**3** isolated from *L. vulgaris*.

PCSK9 can contribute to the buildup of plaque, such as that seen in atherosclerosis.[12,13] Similarly, IDOL binds to the intracellular domain of LDLR, facilitating its ubiquitylation and subsequent lysosomal degradation.[7−11] Thus, it is recognized that a sustained or increased LDLR level in the cell membrane contributes to the lowering of LDLC levels in the blood. By inhibiting PCSK9-mediated LDLR degradation, two antibody drugs and one siRNA drug have been approved for clinical use in treating high blood LDLC levels.[14,15] Therefore, the regulators of PCSK9-mediated LDLR degradation via inhibition of PCSK9-LDLR binding or PCSK9 synthesis have been investigated.

Our ongoing project has been to discover small molecules from edible and medicinal plants with inhibitory activity against PCSK9 mRNA expression.[16−18] During this project, it was found that the hexane-soluble extract of *L. vulgaris* roots inhibited PCSK9 mRNA expression, increasing LDLR mRNA expression (Figure S1). To date, there are no reports regarding the identification of PCSK9 mRNA expression inhibitors from *L. vulgaris*. In this study, two new naturally occurring compounds and 20 known structures (Figure S2) were identified and their effects on PCSK9 and LDLR mRNA expression in HepG2 cell lines were evaluated (Figure 1).

2. RESULTS AND DISCUSSION

Compound **1** was obtained as an amorphous solid, and its molecular formula was determined to be $C_{26}H_{36}O_4$ via high-resolution electrospray ionization mass spectrometry (HRESIMS) using the $[M - H]^-$ ion at m/z 411.2534. The ^{1}H NMR data of **1** displayed a signal for a hydroxy group at δ_H 11.15 (1H, s, 8-OH), a signal derived from an olefinic proton at δ_H 6.15 (1H, s, H-4), and two signals for a tetra-substituted aromatic ring at δ_H 6.38 (1H, brs, H-7) and 6.26 (1H, brs, H-5), indicating the presence of an isocoumarin moiety. The remaining signals were determined to be four unsaturated fatty acid protons at δ_H 5.36 (4H, overlapped, H-8, 9, 11, and 12); 12 methylene protons at δ_H 2.77 (2H, t, J = 7.7 Hz, H-10′), 2.48 (2H, J = 7.7 Hz, H-1′), 2.05 (4H, m, H-7 and 13), 1.66 (2H, m, H-2′), and 1.25−1.39 (14H, overlapped, H-3′-6′ and H-14′-16′); and a methyl proton at δ_H 0.88 (3H, t, J = 7.1 Hz, H-17′), suggestive of an octadecadienyl moiety. The linkage between the isocoumarin and octadecadienyl moieties was found at C-3 by observing the heteronuclear multiple bond correlations (HMBCs) of δ_H 2.48 (H-1′) to δ_C 158.3 (C-3), 103.7 (C-4), 29.4 (C-3′), and 26.8 (C-2′) and δ_H 1.66 (H-2′) to δ_C 158.6 (C-3). In addition, the HMBCs of δ_H 11.15 (8-OH) to δ_C 163.8 (C-8), 102.1 (C-7), and 100.2 (C-9) and the HMBCs of δ_H 6.26 (H-5) to δ_C 163.1 (C-6), 103.7 (C-4), 102.1 (C-7), and 100.2 (C-9) enabled the assignment of a 6,8-dihydroxy-isocoumarin moiety (Figure 2). Moreover, the long-range HMBC ($J_{H,C}$ = 2 Hz) of δ_H 6.26 (H-5) to δ_C 166.4 (C-1) supported the presence of a carbonyl carbon at C-1 (Figures 2 and S11). Therefore, compound **1** was characterized as 8′*Z*,11′*Z*-octadecadienyl-6,8-dihydroxyisocoumarin.

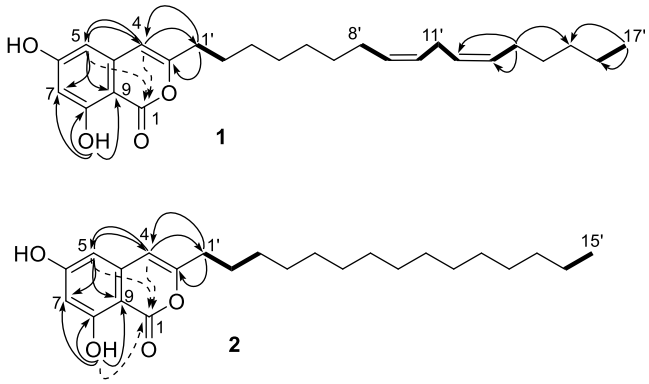

Figure 2. Key ^{1}H-^{1}H COSY (**bold line**), HMBC (**solid arrow**), and long-range HMBC (**dashed arrow**) correlations of compounds **1** and **2**.

The molecular formula of compound **2** was determined to be $C_{24}H_{36}O_4$ by the $[M - H]^-$ ion at m/z 387.2529 in the HRESIMS. The ^{1}H NMR data of **2** displayed nearly identical signals to **1** for 6,8-dihydroxyl-isocoumarin at δ_H 10.96 (1H, s, H-8), 10.84 (1H, s, 6-OH), 6.48 (1H, s, H-4), 6.36 (1H, d, J = 2.1 Hz, H-5), and 6.31 (1H, d, J = 2.1 Hz, H-7). However, there were different signals in the side chain of **2** compared to those of **1**. In **2**, methylene and methyl signals, accounting for the saturated fatty acid, appeared at δ_H 2.47 (2H, t, J = 7.5 Hz, H-1′), 1.58 (2H, m, H-2′), and 1.22−1.29 (24H, overlapped, H-3′-14′) from 14 methylene protons and at δ_H 0.85 (3H, t, J = 7.1 Hz, H-15′) from a methyl proton. The HMBCs of δ_H 2.47 (H-1′) to δ_C 157.3 (C-3), 103.7 (C-4), 28.3 (C-3′), and 26.2 (C-2′) and δ_H 1.58 (H-2′) to δ_C 157.3 (C-3) provided evidence that the saturated fatty acid is connected at C-3 of isocoumarin via a *C*-linkage. Further assignments were accomplished by the HMBCs of δ_H 10.96 (8-OH) to δ_C 162.7 (C-8), 101.4 (C-7), and 98.1 (C-9); δ_H 10.84 (6-OH) to δ_C 165.5 (C-6), 102.6 (C-5), and 101.4 (C-7); δ_H 6.36 (H-5) to δ_C 165.5 (C-6), 103.7 (C-4), 101.4 (C-7), and 98.1 (C-9). Furthermore, the long-range HMBCs ($J_{H,C}$ = 2 Hz) of δ_H 6.36 (H-5) to δ_C 165.4 (C-1) and δ_H 10.96 (8-OH) to δ_C 165.4 (C-1) supported the presence of a carbonyl carbon at C-1 (Figures 2 and S20). Therefore, the structure of **2** was determined to be 3-pentadecyl-6,8-dihydroxyisocoumarin, a compound that has previously been reported in its synthetic form,[19] but has yet to be described as a natural structure.

The known structure compounds (**3**-**22**) were identified by comparison of their spectroscopic data with the reported values, as 5-*O*-methylembelin (**3**),[20] 5-*O*-methylrapanone (**4**),[21] 9-hydroxy-(9*S*,10*E*,12*Z*,15*Z*)- octadecatrienoic acid

https://doi.org/10.1021/acsomega.2c06660
ACS Omega 2022, 7, 47296−47305

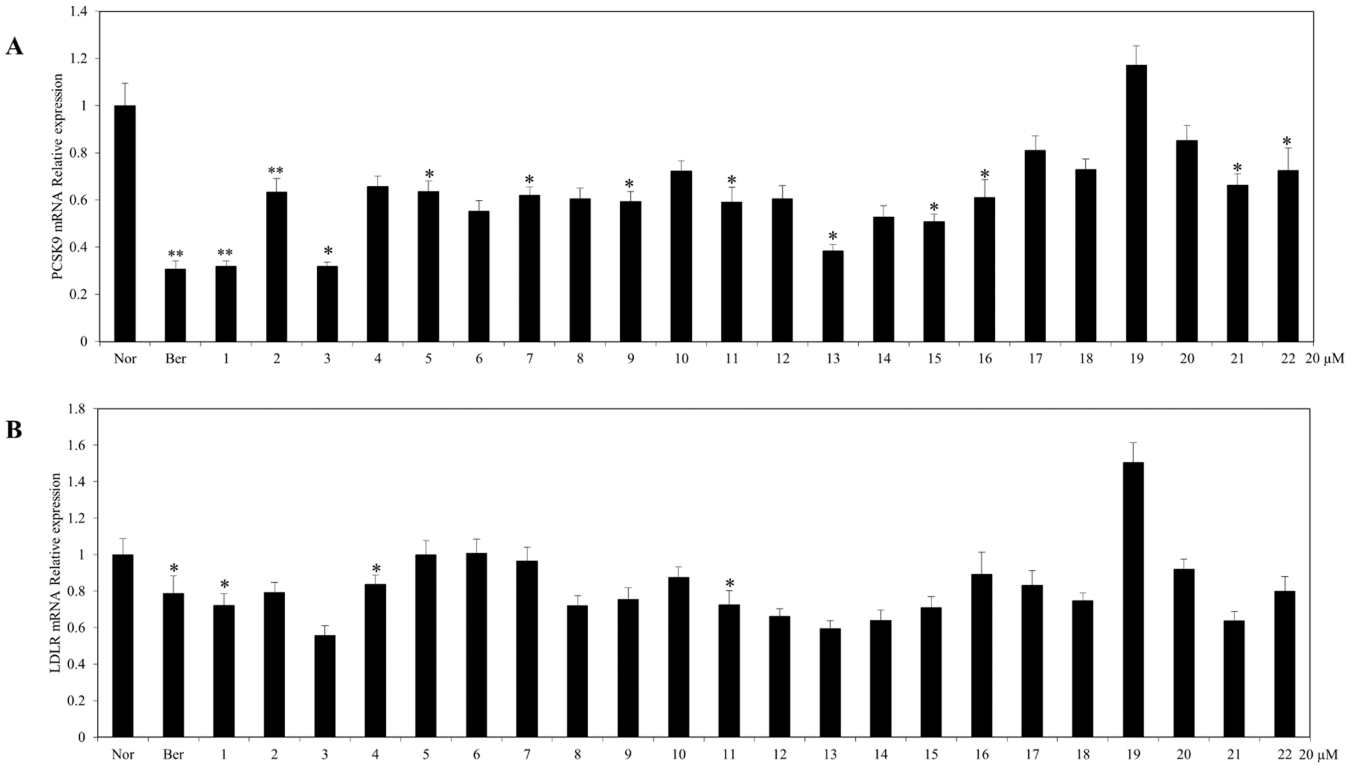

Figure 3. Effects of compounds **1**−**22** on the PCSK9 and LDLR mRNA expressions in the HepG2 cells. (A). Expression of PCSK9 mRNA was assayed by qRT-PCR in cells treated with compounds **1**−**22** (20 μM), and berberine 20 μM (Ber) for 24 h. (B) Expression of LDLR mRNA was assayed by qRT-PCR in cells treated with compounds **1**−**22** (20 μM), and berberine 20 μM (Ber) for 24 h. ** $p < 0.01$ and * $p < 0.05$ as compared to the nontreated group by Dunnett's *t*-test.

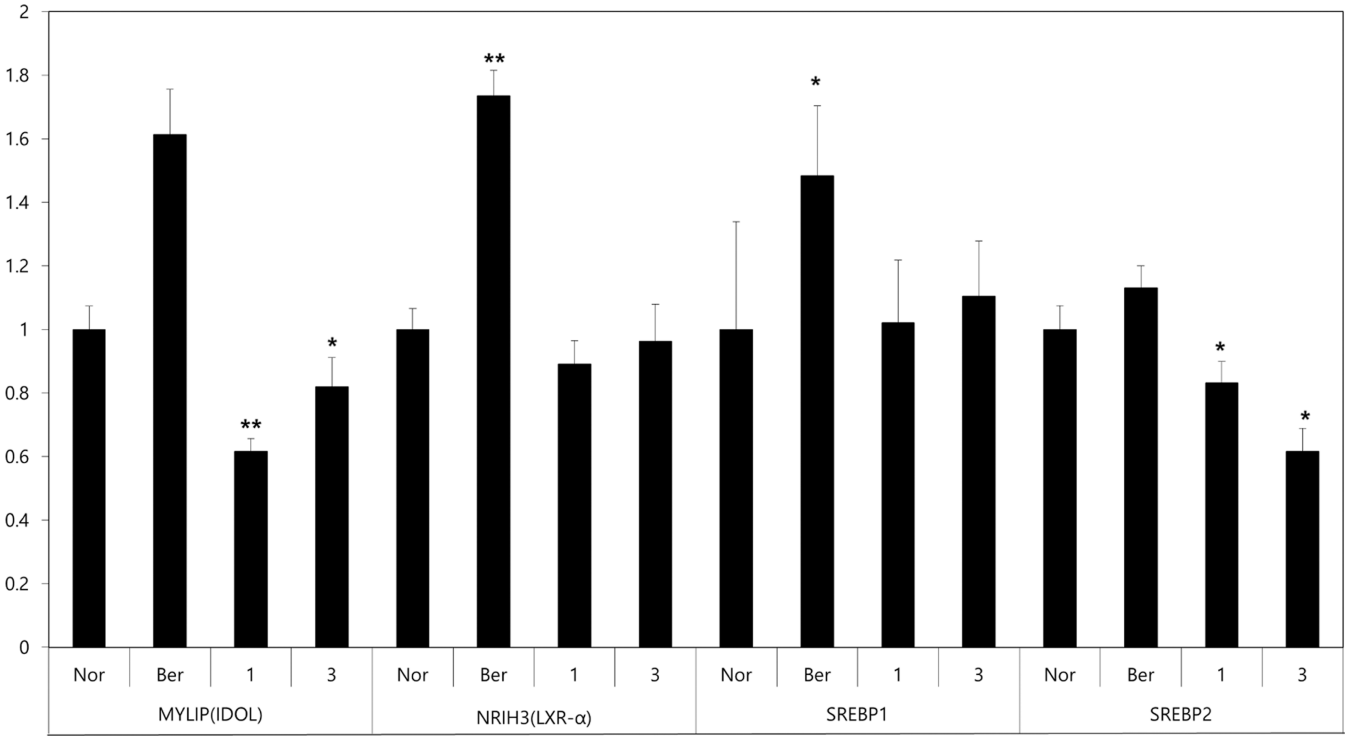

Figure 4. Effects of compounds **1** and **3** (20 μM) and berberine on the MYLIP (IDOL), NRIH3 (LXR-α), SREBP 1, and SREBP 2 genes expressions in the HepG2 cells. The expressions of MYLIP (IDOL), NRIH3 (LXR-α), SREBP 1, and SREBP 2 were assayed by qRT-PCR in cells treated with compounds **1** and **3** for 24 h. **$p < 0.01$ and *$p < 0.05$ as compared to the nontreated group by Dunnett's *t*-test.

(**5**),[22] 9-oxo-(10*E*,12*E*)-octadecadienoic acid (**6**),[23] 9-oxo-(10*E*,12*Z*)-octadecadienoic acid (**7**),[23] 2,3-dihydroxypropyl-(10*Z*,13*Z*)-nonadecadienoate (**8**),[24] 2,3-dihydroxypropylpentadecadienoate (**9**),[25] 1-monopalmitoyl-*rac*-glycerol (**10**),[26]

https://doi.org/10.1021/acsomega.2c06660
ACS Omega 2022, 7, 47296−47305

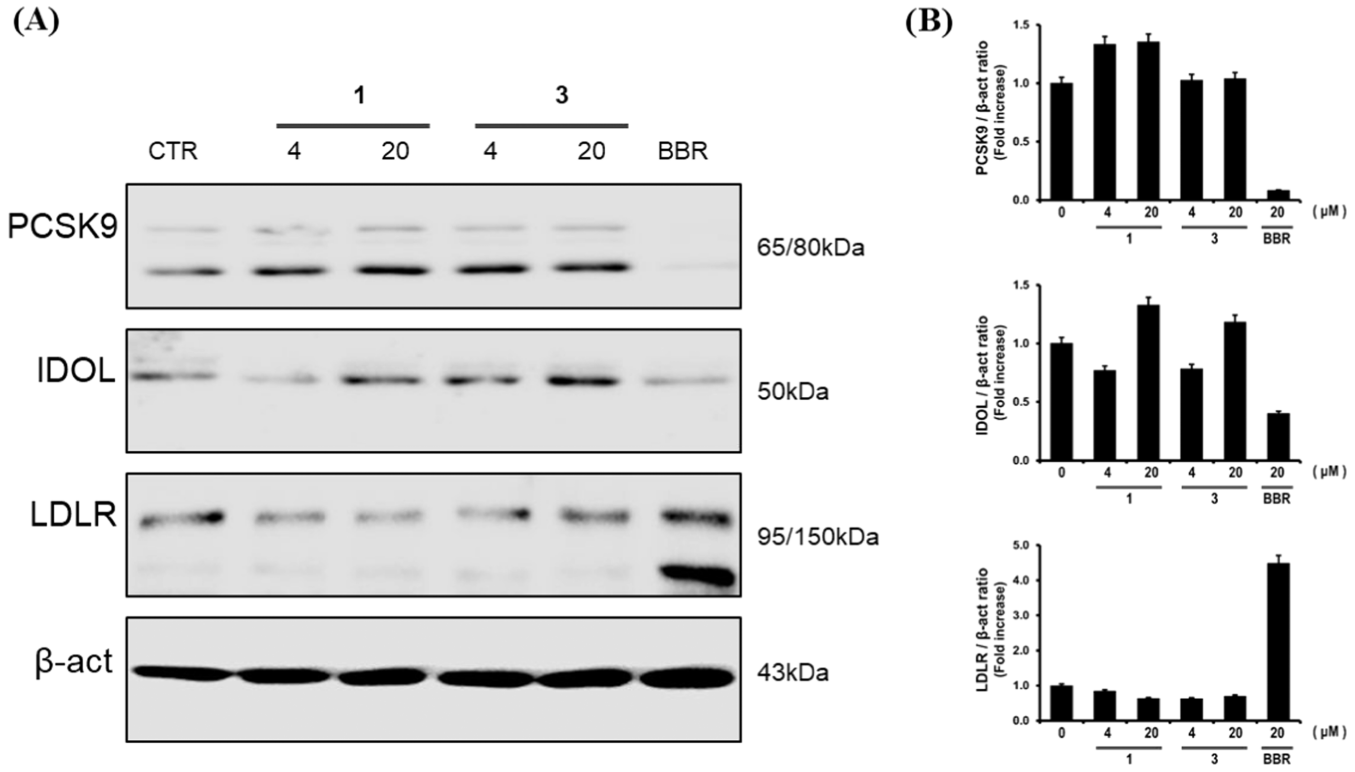

Figure 5. (A) Effects of **1** and **3** on IDOL, PCSK9, LDLR, and β−actin expression in HepG2 cells. HepG2 cells were treated with indicated concentrations of **1** and **3** (4, 20 μM) and berberine (**Ber**, 20 μM) for 24 h. The expression of IDOL, PCSK9 LDLR, and β−actin was examined by western blot analysis. (B) Immunoblot signals were quantified using ImageJ software (NIH, Bethesda, MD).

monononadecanoin (**11**),[27] methyl linoleate (**12**),[6] linoleic acid (**13**),[6] oleic acid (**14**),[24] capric acid (**15**),[28] lauric acid (**16**),[29] palmitic acid (**17**),[30] stearic acid (**18**),[31] (+)-demethoxylpinoresinol (**19**),[6] (+)-pinoresinol (**20**),[6] *trans*-cinnamic acid (**21**),[32] and *cis*-ferulic acid (**22**).[33] The known compounds (**3**-**22**) were isolated from *L. vulgaris* for the first time (Figure S2).

Isocoumarins are commonly found in many natural sources including insects, microorganisms, and plants.[5] However, there are several studies reporting more unusual isocoumarins with 3-alkyl side chains from other natural sources, such as lichens,[34,35] mosses,[36,37] plants,[38−44] and yeast.[45] Although found in many plants,[38−44] only three different 3-alkyl isocoumarins, 8-hydroxy-6-methoxy-3-pentylisocoumarin,[38−44] 6-8-dimethoxy-3-pentylisocoumarin,[41,45] and 7-chloro-8-hydroxy-6-methoxy-3-pentylisocoumarin,[44] have been described to date. Thus far, there are only a few reports investigating these unusual isocoumarins with 3-alkyl side chains and their pharmacological roles.

All compounds isolated from the roots of *L. vulgaris* in the present study were examined for their effects on PCSK9 and LDLR mRNA expressions in human HepG2 cells (Figure 3). Two compounds, 8′*Z*,11′*Z*-octadecadienyl-6,8-dihydroxyisocoumarin (**1**) and 5-*O*-methylembelin (**3**), downregulated PCSK9 mRNA expression significantly at a concentration of 20 μM compared with the untreated group. We further tested these two compounds at a range of concentrations (1.25−20 μM) for their inhibition of PCSK9 mRNA expression in HepG2 cells and found that 8′*Z*,11′*Z*-octadecadienyl-6,8-dihydroxyisocoumarin (**1**) and 5-*O*-methylembelin (**3**) inhibited PCSK9 mRNA expression with IC_{50} values of 11.9 and 4.9 μM, respectively (positive control, berberine chloride, IC_{50} = 3.6 μM).

Consequently, these active compounds, 8′*Z*,11′*Z*-octadecadienyl-6,8-dihydroxyisocoumarin (**1**) and 5-*O*-methylembelin (**3**), were selected to further investigate their effect on LDLR-related genes, including IDOL, liver X receptor (LXR), sterol regulatory element binding protein 1 (SREBP1), and SREBP2. As shown in Figure 4, compounds **1** and **3** appeared to inhibit PCSK9 mRNA expression via downregulation of the transcriptional factor SREBP2. Upregulation of SREBP2 has been known to activate PCSK9 expression in the HepG2 hepatocytes.[46−48] Hence, it can be inferred that inhibition of SREBP2 enables the downregulation of PCSK9 expression, increasing LDL uptake.[46−48] Moreover, the current study demonstrated that 8′*Z*,11′*Z*-octadecadienyl-6,8-dihydroxyisocoumarin (**1**) and 5-*O*-methylembelin (**3**) slightly downregulate IDOL mRNA expression. In contrast, LXRs induce the transcriptional expression of IDOL, which is involved in degrading LDLR and thereby inhibiting LDL uptake.[7−11]

As described in the literature,[7−11] the degradation of LDLR is regulated by two distinctive protein bindings, PCSK9-LDLR binding or IDOL-LDLR binding. Therefore, we assessed **1** and **3** for their inhibitory effect on the protein expression of PCSK9 and IDOL. Contrary to the results of mRNA expression, **1** and **3** slightly upregulated IDOL and the mature form of PCSK9 protein levels in a dose-dependent manner. However, changes in the LDLR protein level were not detected after treatment (Figure 5). Previous studies have reported that several natural products with PCSK9 expression downregulatory activities, including stilbene, xanthone, and triterpenoid, increased LDLR protein levels and subsequent LDL uptake, potentially lowering the LDL cholesterol level.[17,49−52] In addition, some

https://doi.org/10.1021/acsomega.2c06660
ACS Omega 2022, 7, 47296−47305

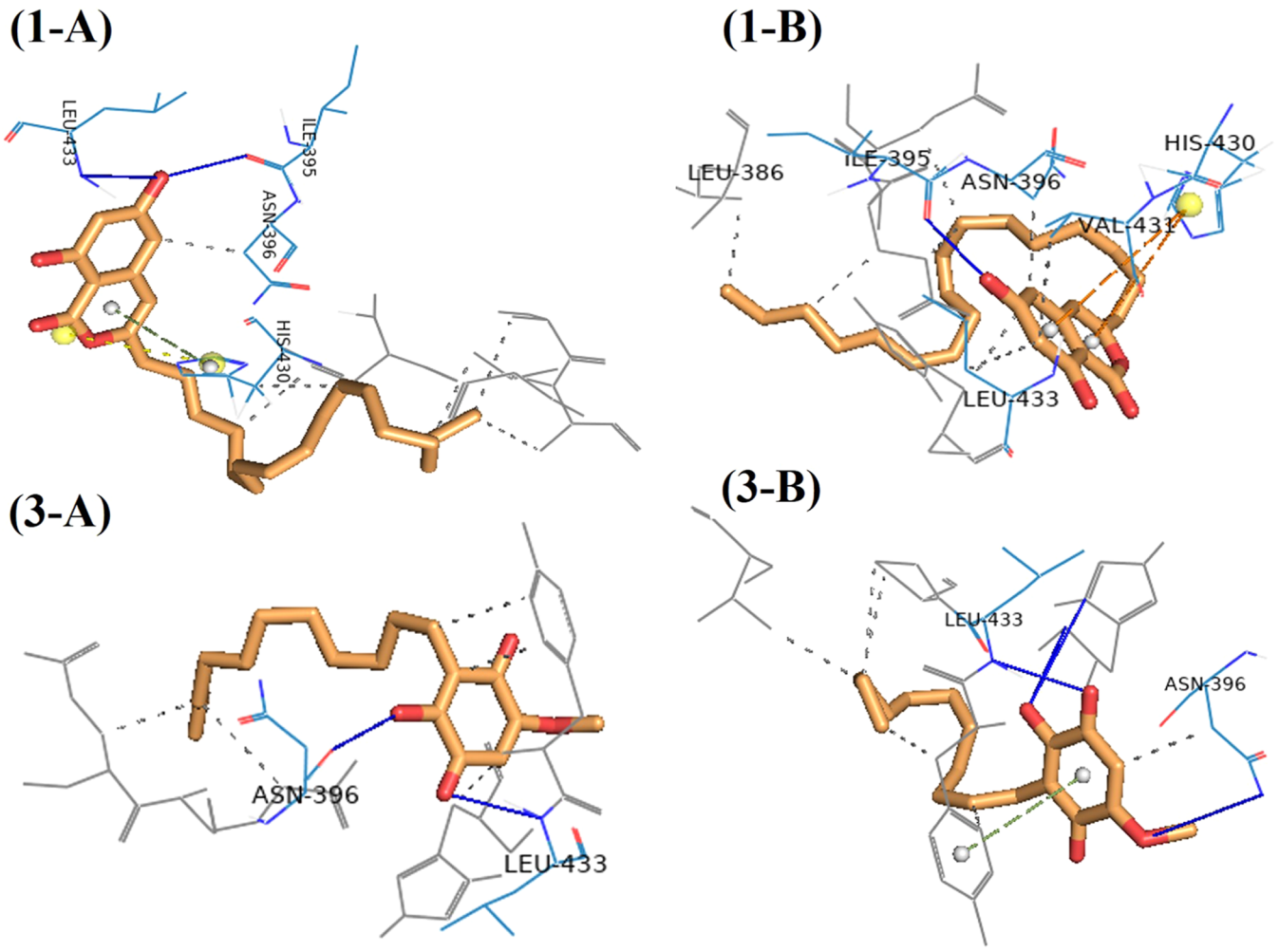

Figure 6. 3D interaction plot of ligand and protein. Binding affinity of **1** with (**1-A**) monomer and (**1-B**) homodimer, and **3** with (**3-A**) monomer and (**3-B**) homodimer are shown.

Table 1. Docking Results of 1 and 3 against Key Sites of IDOL C-Ring Using AutoDock

protein (cluster)	ligand (compounds)	binding energy (Kcal/mol)	ligand efficiency	inhibition constant, K_i (μM)	number of H-bonds and Interacting key proteins
2yhnM (1)	**1**	−6.88	−0.23	9.1	**H-bonds: 2** **AA's:** Ile395, Asn396, His430, Leu433
2yhnHD (3)	**1**	−6.27	−0.21	25.33	**H-bonds: 1** **AA's:** Ile395, Asn396, His430, Val431, Leu433
2yhnHD (1)	**1**	−6.99	−0.23	7.46	**H-bonds: 3** **AA's:** His430, Leu433
2yhnM (2)	**3**	−5.74	−0.26	62.04	**H-bonds: 2** **AA's:** Asn396, Leu433
2yhnM (1)	**3**	−7.01	−0.32	7.3	**H-bonds: 3** **AA's:** Ile395
2yhnHD (1)	**3**	−6.62	−0.30	14.02	**H-bonds: 4** **AA's:** Asn396, Leu433

natural compounds with IDOL expression inhibitory activities, such as platycodin D and xanthohumol, increased the LDLR protein level as well.[8,52]

Since increasing the PCSK9 and IDOL protein levels did not lead to a decrease in the LDLR protein level, computational dockings of both **1** and **3** to the C-ring of IDOL E3 ubiquitin ligase (PDB ID = 2YHN) using AutoDock 1.5.7. were performed to predict their inhibitory activity on the enzyme. Based on previous studies that explored specific amino acid residues involved in the homodimerization of an IDOL ring, five target proteins are known to play key roles in inhibiting this process. First, defective mutant strains of Val431 and Leu433 inhibit IDOL-induced LDLR degradation.[53] Second, three residues, Ile395, Asn396, and His430, are involved in the protein−protein interaction of the homodimerized RING domains of IDOL.[54] Results of the three-dimensional (3D) interactions at the binding site of homodimer (2yhnHD) and monomer (2yhnM) are shown in Figure 6.

https://doi.org/10.1021/acsomega.2c06660
ACS Omega 2022, 7, 47296−47305

Four target amino acid residues from the monomer (2yhnM) interacted with **1** through various means. Hydrogen bonds were formed between 6-OH and two residues (Ile395 and Leu433). Hydrophobic interaction was also identified between Asn396 and C-5. His430 formed various interactions including a hydrophobic interaction (C-11′) and a salt bridge and stacking with a ring of the ligand.

Despite the better binding energy and inhibition constant of cluster rank 1, a larger number of key interactions were observed from the structural configuration in cluster rank 3 (Table 1). All five target residues from 2yhnHD showed at least one interaction with **1**, supported by the exact same hydrogen bond formed by Ile395 as seen with the monomer. Three hydrophobic interactions with Asn396, Val431, and Leu433 were also detected at different positions of the ligand. His430 exhibited stacking with both rings of **1**.

Similar to above, the interaction of cluster rank 2 of compound **3** with the monomer showed a wider range of different interactions than that of cluster rank 1. Two hydrogen bonds were established, one between Asn396 and 6-OH and the other between Leu433 and the ketone group at C-5. Likewise, **3** expressed two hydrogen bonds with 2yhnHD, just like those with the monomer, except the direction of bonding of Asn396 was changed to the 3-methoxy group. Other key values, including binding energy, are recorded in Table 1.

To gain further support for the results above, dockings were also conducted for RINGPep1 and RINGPep2 (Figure S21), two newly synthesized compounds that are known to be effective in inhibiting IDOL E3 ubiquitin ligase by interrupting homodimerization.[54] RINGPep1 and RINGPep2 were used as reference ligands because they are known to have high binding affinities through low dissociation constant (Kd) values.[54] A 3D visualization of interactions between ligand and protein is shown in Figure S21. More hydrogen bonds were identified in the docking simulation between RINGPep1 and the monomer than RINGPep2 and the monomer, although participation by key target proteins in the interaction was not so different from those seen with **1** and **3**. In addition, lower binding energies and very low inhibition constants for RINGPep1 and RINGPep2 were observed using AutoDock as shown in Table S1, which are comparable to their calculated dissociation constants from the original study.[54]

Low binding energies, supported by negative ligand efficiency values and inhibition constants, indicate high binding affinities of **1** and **3** with the target residues. Both the monomer and homodimer were tested to identify the effect of the ligand in preventing and disrupting homodimerization, respectively. According to the results, **1** and **3** have low binding energies and inhibition constants, with a greater number of interactions between target proteins and both **1** and **3**. This finding may, in part, explain the negligible change of LDLR protein level.

3. CONCLUSIONS

In this study, we found two new isocoumarins, 8′*Z*,11′*Z*-octadecadienyl-6,8-dihydroxyisocoumarin (**1**) and 3-pentadecyl-6,8-dihydroxyisocoumarin (**2**), along with 20 known compounds in the hexane-soluble fraction of *L. vulgaris*. Of these compounds, **1** and **3** inhibited PCSK9, IDOL, and SREBP2 mRNA expression. While compounds **1** and **3** did not increase LDLR protein level in this study, a docking simulation of **1** and **3** on homodimerization of IDOL E3 ubiquitin ligase suggested these compounds may interrupt homodimerization and prevent the function of IDOL E3 ubiquitin ligase, which may in part propose a plausible mechanism of action of these compounds.

4. EXPERIMENTAL SECTION

4.1. General Experimental Procedures. The JASCO P-2000 digital polarimeter (Jasco, Tokyo, Japan) was used to perform the optical rotations. Ultraviolet−visible spectra were measured by a Chirascan Plus circular dichroism spectrometer (APL, Surrey, UK). Fourier transform infrared (FT-IR) spectroscopy was performed on a Thermo Fisher Scientific, Nicolet iS 5 FT-IR spectrometer (Thermo Fisher Scientific, Wisconsin). Nuclear magnetic resonance (NMR) spectra were recorded on Bruker AVANCE 400 and Bruker AVANCE 500 spectrometers (Bruker, Karlsruhe, Germany). High-resolution mass spectra data were performed using a Waters Xevo G2 Q-TOF mass spectrometer (Waters, Medford, MA). Semi-preparative high-performance liquid chromatography (HPLC) was performed on a Gilson 321 pump and Gilson 172 Diode Array Detector (Gilson, Madison, WI) and YMC-pack Ph, 250 mm × 10 mm (YMC. Kyoto, Japan) column was used. Medium-pressure liquid chromatography was subjected to Biotage Isolera one (Biotage, Uppsala, Sweden) with C-18 RP silica gel (Cosmosil, Kyoto, Japan). Water was purified using a Milli-Q system (Water Corporation, Milford, MA). Column chromatography was performed on silica gel (Cosmosil, Kyoto, Japan). Thin-layer chromatography (TLC) analysis was conducted on silica gel 60 F_{254} and silica gel RP-C_{18} plates (Merck, Darmstadt, Germany). The spots were visualized by spraying 10% aqueous H_2SO_4.

4.2. Reagents. Solvents for extraction and isolation (methanol, *n*-hexane, chloroform, ethyl acetate, *n*-butanol, acetonitrile (MeCN) (HPLC grade) and methanol (HPLC grade), etc.) were purchased from SK Chemical (Seoul, Korea). The solvents for NMR ($CDCl_3$) and (CD_3OD) were purchased from Cambridge Isotope Laboratories, Inc. (Andover, MA).

4.3. Plant Material. The dried roots (1.6 kg) of *L. vulgaris* were harvested at Eumseong County in August 2017 and identified by Jeong Hoon Lee. A voucher specimen has been deposited at the Department of Herbal Crop Research, National Institute of Horticultural and Herbal Science (Voucher No. MPS000991), Republic of Korea.

4.4. Extraction and Isolation. The dried roots (1.6 kg) were extracted with 100% MeOH at room temperature three times. The crude extract (86.0 g) was obtained. The extract was suspended with 1.0 L of H_2O in partition flesh. The partitions were repeated three times with organic solvents: *n*-hexane, ethyl acetate, giving the residues of *n*-hexane-soluble extract (5.6 g), ethyl acetate-soluble (6.2 g), and water-soluble extract (63.8 g).

The *n*-hexane-soluble extract (5.2 g, LVH) was chromatographed on silica column chromatography with gradient mixtures of *n*-hexane and ethyl acetate (20:1 to 1:1) then $CHCl_3$−MeOH (20:1 to 2:1), to afford 9 subfractions (LVH-1 to LVH-9). The fraction LVH-2 (15.7 mg) was purified on HPLC (MeCN-H_2O 50%, isocratic elution, 3.0 mL/min) to give **12** (t_R 19.5 min, 4.0 mg). The LVH-5 fraction (826.2 mg) was subjected on MPLC run using a reversed-phase silica gel (50 g) column with MeOH-H_2O (20:80 to 80:20), giving eight subfractions (LVH-5A to LVH-5H). The LVH-5A fraction (31.0 mg) was separated on semipreparative HPLC (MeCN-H_2O 35%, isocratic elution, 3.0 mL/min) for 15 min,

https://doi.org/10.1021/acsomega.2c06660
ACS Omega 2022, 7, 47296−47305

to produce **22** (t_R 13.02 min, 1.2 mg). Using the HPLC separation (MeCN-H_2O 65%, isocratic elution, 3.0 mL/min), **16** (t_R 9.9 min, 1.7 mg), **17** (t_R 15.6 min, 5.1 mg), and **18** (t_R 18.6 min, 1.7 mg) were isolated from the LVH-5E subfraction (39.9 mg), and the same method was applied on the LVH-5F fraction (50.5 mg), to afford **14** (t_R 20.0 min, 7.7 mg) and **13** (t_R 29.8 min, 3.6 mg). The LVH-6 fraction (71.2 mg) was purified on semipreparative HPLC (MeCN-H_2O 75%, isocratic elution, 3.0 mL/min), to yield **3** (t_R 23.0 min, 10.1 mg) and **4** (t_R 31.7 min, 2.6 mg). The LVH-7 fraction (40.3 mg) was further purified on HPLC separation (MeCN-H_2O 30 to 70%, gradient elution, 3.0 mL/min) for 20 min, to produce **20** (t_R 12.4 min, 1.8 mg), **1** (t_R 17.8 min, 2.0 mg), and **2** (t_R 19.3 min, 6.7 mg). The LVH-8 fraction (115.2 mg) gave **19** (t_R 17.7 min, 1.2 mg), **21** (t_R 18.8 min, 1.6 mg), **5** (t_R 28.0 min, 1.1 mg), **15** (t_R 29.0 min, 5.0 mg), **6** (t_R 30.2 min, 1.9 mg), **7** (t_R 30.9 min, 2.1 mg), **9** (t_R 33.7 min, 2.5 mg), **8** (t_R 36.2 min, 1.6 mg), **10** (t_R 37.3 min, 1.5 mg), and **11** (t_R 38.2 min, 2.0 mg) by HPLC separation (MeCN-H_2O 10 to 100%, gradient mood for 30 min, and then 100%, isocratic mode for 10 min, 3.0 mL/min).

4.5. Quantitative Real-Time PCR. PCR analysis was performed according to the previously reported method.[16−18] The following specific primer sets were used (5′ to 3′): GAPDH: GAAGGTGAAGGTCGGAGTCA (forward), AATGAAGGGGTCATTGATGG (reverse); PCSK9GGGCATTTCACCATTCAAAC (forward), TCCAGAAAGCTAAGCCTCCA (reverse); IDOL(MYLIP): ACGGTCACCAAGGAATCTGGGA (forward), CCTTCAAGTCACGGCTATACTGC (reverse); LXR-α-(NR1H3): TGGACACCTACATGCGTCGCAA (forward), CAAGGATGTGGCATGAGCCTGT (reverse); SREBP1: ACTTCTGGAGGCATCGCAAGCA (forward), AGGTTCCAGAGGAGGCTACAAG (reverse) and SREBP2: CTCCATTGACTCTGAGCCAGGA (forward), GAATCCGTGAGCGGTCTACCAT (reverse). Gene-specific primers were custom-synthesized by Bioneer (Daejeon, Korea).

4.6. Western Blot. HepG2 cells were lysed in RIPA buffer containing Xpert Protease Inhibitor and Phosphatase Inhibitor Cocktail Solution (GenDEPOT) on ice for 10 min. Cell lysates were centrifuged at 14,000 rpm for 15 min at 4 °C, and supernatants were quantified using the Pierce BCA Protein Assay Kit (Thermo Fisher Scientific, Inc.). Proteins were separated by electrophoresis on a 10% sodium dodecyl sulfate-polyacrylamide gel (SDS-PAGE) and were transferred onto polyvinylidene difluoride (PVDF) membrane. The membrane was treated with 3% skimmed milk for 1 h and incubated overnight at 4 °C with primary antibodies in 3% bovine serum albumin (BSA). After washing with Tris-buffered saline with 0.1% Tween 20 (TBST), the membrane was incubated with the HRP-conjugated secondary antibody (1:5000) for 1 h at room temperature. The band images were acquired using a ChemiDoc Imaging system (Bio-Rad) using West-Q ECL Solution (GenDEPOT).

4.7. AutoDock Methods. The homodimer protein structure of IDOL-E3 ring (PDB ID: 2yhn) was downloaded from RCSB Protein Data Bank. PyMOL was used to remove unwanted small molecules (Zn^{2+}), as well as chain B to obtain monomer. Preparation of protein, including filling in missing atoms and adding polar hydrogens, was conducted using AutoDock. AutoDock Tools 1.5.7 was used to simulate the docking of ligands of interest against the prepared proteins. For docking parameter, grid dimensions of 60 × 60 × 60 points and a grid of spacing of 0.375 Å were instrumented for both 2yhnHD and 2yhnM. The calculation involved 50 runs of the Lamarckian genetic algorithm with 25,000,000 evaluations and 27,000 generations. Visualization of binding affinity between ligands and residues was performed with 'Protein-Ligand Interaction Profiler' and PyMOL.[55]

4.8. Statistical Analysis. Data from the experiments are presented as the mean ± S.E.M. The level of statistical significance was determined by one-way analysis of variance (ANOVA) and Dunnett's *t*-test for multiple comparisons. *P* values less than 0.05 were considered significant.

4.8.1. 8′Z,11′Z-Octadecadienyl-6,8-dihydroxyisocoumarin (1). Amorphous solid, UV λ_{max}^{MeOH} (log ε): 242.0 (3.26), 327.0 (2.48). FT-IR (ATR) ν_{max} 2925, 2856, 1680, 1626, 1460, 1368, 1238, 1169 cm^{-1}. ^1H NMR (CD_3OD, 400 MHz) δ 11.15 (1H, s, 8-OH), 6.38 (1H, brs, H-7), 6.26 (1H, brs, H-5), 6.15 (1H, s, H-4), 5.36 (4H, m, H-8′, 9′, 11′ and 12′), 2.77 (2H, t, J = 7.7 Hz, H-10′), 2.48 (2H, s, J = 7.7 Hz, H-1′), 2.05 (4H, m, H-7′ and 13′), 1.66 (2H, m, H-2′), 1.25−1.39 (14H, overlapped, H- 3′−6′ and H-14′−16′), and 0.88 (3H, t, J = 7.1 Hz, H-17′); ^{13}C NMR (CD_3OD, 100 MHz) δ 166.4 (C-1), 163.8 (C-8), 163.1 (C-6), 158.3 (C-3), 140.0 (C-10), 130.3 (C-8′), 130.1 (C-11′), 128.1 (C-9′), 127.9 (C-12′), 103.7 (C-4), 102.1 (C-7), 101.8 (C-5), 100.2 (C-9), 33.3 (C-1′), 31.5 (C-15′), 29.6 (C-14′), 29.4 (C-3′), 29.2 (C-4′), 29.1 (C-5′), 29.1 (C-6′), 27.2 (C-7′ and C-13′), 26.8 (C-2′), 25.6 (C-10′), 22.3 (C-16′), and 14.1 (C-17′). HRESIMS m/z $[M\text{-}H]^-$ 411.2534 (calcd for $C_{26}H_{35}O_4$ 411.2535).

4.8.2. 3-Pentadecyl-6,8-dihydroxyisocoumarin (2). Amorphous solid, UV λ_{max}^{MeOH}(log ε): 241.0 (3.55), 327 (2.78). FT-IR (ATR) ν_{max} 3541, 2914, 2852, 1682, 1637, 1476, 1362, 1241, 1175 cm^{-1}. ^1H NMR (CD_3OD,500 MHz) δ 10.96 (1H, s, 8-OH), 10.84 (1H, s, 6-OH), 6.48 (1H, s, H-4), 6.36 (1H, d, J = 2.1 Hz, H-5), 6.31 (1H, d, J = 2.1 Hz, H-7), 2.47 (2H, t, J = 7.5 H-1′), 1.58 (2H, m, J = 7.7 Hz, H-2′), 1.22−1.29 (24H, overlapped, H- 3′−14′), and 0.85 (3H, t, J = 7.1 Hz, H-15′); ^{13}C NMR (CD_3OD, 125 MHz) δ 165.7 (C-1), 165.5 (C-6), 162.7 (C-8), 157.3 (C-3), 139.6 (C-10), 103.7 (C-4), 102.6 (C-5), 101.7 (C-7), 98.1 (C-9), 32.3 (C-1′), 31.3 (C-13′), 29.2 (C-12′), 29.1 (C-4′ and C-11′), 29.0 (C-5′ and C-10′), 28.9 (C-6′), 28.8 (C-7′), 28.7 (C-8′), 28.6 (C-9′), 28.3 (C-3′), 22.1 (C-14′), and 13.9 (C-15′). HRESIMS m/z $[M - H]^-$ 387.2529 (calcd for $C_{24}H_{35}O_4$ 387.2535).

■ ASSOCIATED CONTENT

Supporting Information

The Supporting Information is available free of charge at https://pubs.acs.org/doi/10.1021/acsomega.2c06660.

Effects of extracts of *Lysimachia vulgaris* on the PCSK9 and LDLR mRNA expressions in the HepG2 cells; UV, HRESIMS, IR, 1D, and 2D NMR spectra for **1**, and **2** (PDF)

■ AUTHOR INFORMATION

Corresponding Author

Young-Won Chin − *College of Pharmacy and Research Institute of Pharmaceutical Sciences, Seoul National University, Seoul 08826, Republic of Korea;* orcid.org/0000-0001-6964-1779; Phone: +82-2-880-7859; Email: ywchin@snu.ac.kr

https://doi.org/10.1021/acsomega.2c06660
ACS Omega 2022, 7, 47296−47305

Authors

Pisey Pel − *College of Pharmacy and Research Institute of Pharmaceutical Sciences, Seoul National University, Seoul 08826, Republic of Korea*

Young-Mi Kim − *College of Pharmacy and Research Institute of Pharmaceutical Sciences, Seoul National University, Seoul 08826, Republic of Korea;* orcid.org/0000-0002-9443-9393

Hyun Ji Kim − *College of Pharmacy and Integrated Research Institute for Drug Development, Dongguk University-Seoul, Goyang-si, Gyeonggi-do 10326, Republic of Korea*

Piseth Nhoek − *College of Pharmacy and Research Institute of Pharmaceutical Sciences, Seoul National University, Seoul 08826, Republic of Korea*

Chae-Yeong An − *College of Pharmacy and Research Institute of Pharmaceutical Sciences, Seoul National University, Seoul 08826, Republic of Korea*

Min-Gyung Son − *College of Pharmacy and Research Institute of Pharmaceutical Sciences, Seoul National University, Seoul 08826, Republic of Korea*

Hongic Won − *College of Pharmacy and Research Institute of Pharmaceutical Sciences, Seoul National University, Seoul 08826, Republic of Korea*

Seung Eun Lee − *Department of Herbal Crop Research, National Institute of Horticultural and Herbal Science (NIHHS) of Rural Development Administration, Eumseong 27709, Republic of Korea*

Jeonghoon Lee − *Department of Herbal Crop Research, National Institute of Horticultural and Herbal Science (NIHHS) of Rural Development Administration, Eumseong 27709, Republic of Korea*

Hyun Woo Kim − *College of Pharmacy and Integrated Research Institute for Drug Development, Dongguk University-Seoul, Goyang-si, Gyeonggi-do 10326, Republic of Korea*

Young Hee Choi − *College of Pharmacy and Integrated Research Institute for Drug Development, Dongguk University-Seoul, Goyang-si, Gyeonggi-do 10326, Republic of Korea*

Chang Hoon Lee − *College of Pharmacy and Integrated Research Institute for Drug Development, Dongguk University-Seoul, Goyang-si, Gyeonggi-do 10326, Republic of Korea*

Complete contact information is available at: https://pubs.acs.org/10.1021/acsomega.2c06660

Notes

The authors declare no competing financial interest.

■ ACKNOWLEDGMENTS

This research was supported by the National Research Foundation of Korea (NRF) grant funded by the Korea government (MSIT) (NRF-2022R1A2C1010084, Y.-W.C., NRF2018R1A5A2023127). The Basic Science Research Program and the BK21 FOUR program through the NRF (NRF-2018R1A5A2023127).

■ REFERENCES

(1) Turker, A. U.; Guner, B. Efficient plant regeneration of yellow loosestrife (*Lysimachia vulgaris* L.), a medical plant. *Acta Biol. Hung.* **2013**, *64*, 218−230.

(2) Kim, S. Y.; Lee, J. Y.; Jhin, C.; Shin, J. M.; Kim, M.; Ahn, H. R.; Yoo, G.; Son, Y.-J.; Jung, S. H.; Nho, C. W. Reduction of hepatic lipogenesis by loliolide and pinoresinol from *Lysimachia vulgaris* via degrading liver X receptors. *J. Agric. Food Chem.* **2019**, *67*, 12419−12427.

(3) Son, Y.-J.; Jung, D. S.; Shin, J. M.; Kim, M.; Yoo, G.; Nho, C. W. Yellow loosestrife (*Lysimachia vulgaris* var. *davurica*) ameliorates liver fibrosis in *db/db* mice with methionine- and choline- deficient diet-induced nonalcoholic steatohepatitis. *BMC Complementary Med. Ther.* **2021**, *21*, No. 44.

(4) Yildirim, A. B.; Guner, B.; Karakas, F. P.; Turker, A. U. Evaluation of antibacterial, antitumor, antioxidant activities and phenolic constituent of field-grown and *in vitro*-growing *Lysimachia vulgaris* L. *Afr. J. Tradit., Complementary Altern. Med.* **2017**, *14*, 177−187.

(5) Pel, P.; Chae, H.-S.; Nhoek, P.; Yeo, W.; Kim, Y.-M.; Chin, Y.-W. Lignans from the fruits of *Schisandra chinensis* (Turcz.) Baill inhibit proprotein convertase subtilisin/kexin type 9 expression. *Phytochemistry* **2017**, *136*, 119−124.

(6) Pel, P.; Chae, H.-S.; Nhoek, P.; Kim, Y.-M.; Chin, Y.-W. Chemical constituents with proprotein convertase subtilisin/kexin type 9 mRNA expression inhibitory activity from dried immature *Morus alba* fruits. *J. Agric. Food Chem.* **2017**, *65*, 5316−5321.

(7) Strong, A.; Rader, D. J. Clinical implications of lipid genetics for cardiovascular disease. *Curr. Cardiovasc. Risk Rep.* **2010**, *4*, 461−468.

(8) Choi, Y.-J.; Lee, S. J.; Kim, H. I.; Lee, H. J.; Kang, S. J.; Kim, T. Y.; Cheon, C.; Ko, S.-G. Platycodin D enhances LDLR expression and LDL uptake via down-regulation of *IDOL* mRNA in hepatic cells. *Sci. Rep.* **2020**, *10*, No. 19834.

(9) Martinelli, L.; Adamopoulos, A.; Johansson, P.; Wan, P. T.; Gunnarsson, J.; Guo, H.; Boyd, H.; Zelcer, N.; Sixma, T. K. Structural analysis of the LDL receptor-interacting FERM domain in the E3 ubiquitin ligase IDOL reveals an obscured substrate-binding site. *J. Biol. Chem.* **2020**, *295*, 13570−13583.

(10) Wang, J.-Q.; Lin, Z.-C.; Li, L.-L.; Zhang, S.-F.; Li, W.-H.; Liu, W.; Song, B.-L.; Luo, J. SUMOylation of the ubiquitin ligase IDOL decrease LDL receptor levels and is reversed by SENP1. *J. Biol. Chem.* **2021**, *296*, No. 100032.

(11) Liu, S.; Vaziri, N. D. Role of PCSK9 and IDOL in the pathogenesis of acquired LDL receptor deficiency and hypercholesterolemia in nephrotic syndrome. *Nephrol. Dial. Transplant.* **2014**, *29*, 538−543.

(12) Macchi, C.; Ferri, N.; Sirtori, C. R.; Corsini, A.; Banach, M.; Ruscica, M. Proprotein covertase substilisin/kexin type 9 a view beyond the canonical cholesterol-lowering impact. *Am. J. Pathol.* **2021**, *191*, 1385−1397.

(13) Seidah, N. G.; Garçon, D. Expanding biology of PCSK: Roles in atherosclerosis and beyond. *Curr. Atheroscler. Rep.* **2022**, *24*, 821−830.

(14) Talasaz, A. H.; Ho, A.-C.; Bhatty, F.; Koenig, R. A.; Dixon, D. L.; Baker, W. L.; Van Tassell, B. W. Meta-analysis of clinical outcomes of PCSK9 modulators in patients with establish ASCVD. *Phamacotherapy* **2021**, *41*, 1009−1023.

(15) Burger, A. L.; Pogran, E.; Muthspiel, M.; Kaufmann, C. C.; Jäger, B.; Huber, K. New treatment targets and innovative lipid-lowering therapies in very-high-risk patients with cardiovascular disease. *Biomedicines* **2022**, *10*, 970.

(16) Pel, P.; Chae, H.-S.; Nhoek, P.; Kim, Y.-M.; Khiev, P.; Kim, G. J.; Nam, J.-W.; Choi, H.; Choi, Y. H.; Chin, Y.-W. A stilbene dimer and flavonoids from the aerial parts of *Chromolaena odorata* with proprotein convertase sbutilisin/kexin type 9 expression inhibitory activity. *Bioorg. Chem.* **2020**, *99*, No. 103869.

(17) Chae, H.-S.; Pel, P.; Cho, J.; Kim, Y.-M.; An, C.-Y.; Huh, J.; Choi, Y. H.; Kim, J.; Chin, Y.-W. Identification of neolignans with PCSK9 downregulatory and LDLR upregulatory activities from *Penthorum chinense* and the potential in cholesterol uptake by transcriptional regulation of LDLR via SREBP2. *J. Ethnopharmacol.* **2021**, *278*, No. 114265.

(18) Nhoek, P.; Chae, H.-S.; Kim, Y.-M.; Pel, P.; Huh, J.; Kim, H. W.; Choi, Y. H.; Lee, K.; Chin, Y.-W. Sesquiterpenoids from the aerial parts of *Salvia plebeian* with inhibitory activities on proprotein

convertase subtilisin/kexin type 9 expression. *J. Nat. Prod.* **2021**, *84*, 220−229.
(19) Kaji, H.; Yamada, M.; Nozawa, K.; Kawai, K.; Nakajima, S. Synthesis of antifungal isocoumarins. *Org. Prep. Proced. Int.* **1986**, *18*, 253−262.
(20) Omosa, L. K.; Midiwo, J. O.; Mbaveng, A. T.; Tankeo, S. B.; Seukep, J. A.; Voukeng, I. K.; Dzotam, J. K.; Isemeki, J.; Derese, S.; Omolle, R. A.; Efferth, T.; Kuete, V. Antibacterial activities and structure-activity relationships of a panel of 48 compounds from Kenyan plants against multidrug resistant phenotypes. *Springerplus* **2016**, *5*, No. 901.
(21) Dang, P. H.; Nguyen, H. X.; Nguyen, N. T.; Le, H. N. T.; Nguyen, M. T. T. α- glucosidase inhibitors from the stems of *Emlelia ribes*. *Phytother. Res.* **2014**, *28*, 1632−1636.
(22) McLean, S.; Reynolds, W. F.; Tinto, W. F.; Chan, W. R.; Shepherd, V. Complete ^{13}C and ^{1}H spectral assignments of prenylated flavonoids and a hydroxyl fatty acid from the leaves of Caribbean *Artocarpus communis*. *Magn. Reson. Chem.* **1996**, *34*, 719−722.
(23) Takahashi, H.; Kim, Y.-I.; Hirai, S.; Goto, T.; Ohyane, C.; Tsugane, T.; Konishi, C.; Fujii, T.; Inai, S.; Iijima, Y.; Aoki, K.; Shibata, D.; Takahashi, N.; Kawada, T. Comparative and stability analyses of 9- and 13-Oxo-octadecadienoic acids in various species of tomato. *Biosci., Biotechnol., Biochem.* **2011**, *75*, 1621−1624.
(24) Itabashi, Y.; Myher, J. J.; Kuksis, A. High-performance liquid chromatographic resolution of reverse isomers of 1,2-diacyl-*rac*-glycerols as 3,5-dinitrophenylurethanes. *J. Chromatogr. A* **2000**, *893*, 261−279.
(25) Sabudak, T.; Isik, E.; Oksuz, S. Lipid constituents of *Trifolium resupinatum* var. *microcephalum*. *Nat. Prod. Res.* **2007**, *21*, 828−833.
(26) Vollhardt, D.; Brezesinski, G. Phase characteristics of 1-monopalmitoyl-*rac*-glycerol monolayers at the air/water interface. *Langmuir* **2016**, *32*, 7316−7325.
(27) Mei, Q.-X.; Chen, X.-L.; Xia, X.; Fang, Z.-J.; Zhou, H.-B.; Gao, Y.-Q.; Dai, W.-B.; Jiang, R.-W. Isolation and chemotaxonomic significance of chemical constituents from *Rubus parvifolius*. *Chin. Herb. Med.* **2016**, *8*, 75−79.
(28) Khalandi, H.; Masoori, L.; Farahyar, S.; Delbandi, A. A.; Raiesi, O.; Farzanegan, A.; Khalandi, G.; Mahmoudi, S.; Erfanirad, T.; Falahati, M. Antifungal activity of capric acid, nystatin, and fluconazole and their *in vitro* interactions against *Candida* isolates from neonatal oral thrush. *Assay Drug Dev. Technol.* **2020**, *18*, 195−201.
(29) Yamashita, S.; Igarashi, M.; Hayashi, C.; Shitara, T.; Nomoto, A.; Mizote, T.; Shibasaki, M. Identification of self-growth-inhibiting compounds lauric acid and 7-(*Z*)-tetradecenoic acid from *Helicobacter pylori*. *Microbiology* **2015**, *161*, 1231−1239.
(30) Fattore, E.; Fanelli, R. Palm oil and palmitic acid: a review on cardiovascular effects and carcinogenicity. *Int. J. Food Sci. Nutr.* **2013**, *64*, 648−659.
(31) Meng, H.; Matthan, N. R.; Wu, D.; Li, L.; Rodríguez-Morató, J.; Cohen, R.; Galluccio, J. M.; Dolnikowski, G. G.; Lichtenstein, A. H. Comparison of diets enriched in stearic, oleic, and palmitic acids on inflammation, immune response, cardiometabolic risk factors, and fecal bile acid concentrations in mildly hypercholesterolemic postmenopausal women-randomized crossover trial. *Am. J. Clin. Nutr.* **2019**, *110*, 305−315.
(32) Amjaour, H.; Wang, Z.; Mabin, M.; Puttkammer, J.; Busch, S.; Chu, Q. R. Scalable preparation and property investigation of a *cis*-cyclobutane-1,2-dicarboxylic acid from β−*trans*-cinnamic acid. *Chem. Commun.* **2019**, *55*, 214−217.
(33) Horbury, M. D.; Baker, L. A.; Quan, W.-D.; Greenough, S. E.; Stavros, V. G. Photodynamics of potent antioxidants: ferulic and caffeic acids. *Phys. Chem. Chem. Phys.* **2016**, *18*, 17691−17697.
(34) Asai, M.; Hattori, Y.; Makabe, H. Synthesis of isocoumarin compounds, 8-hydroxy-6-methoxy-3-pentyl-*1H*-isochromen-1-one and fusariumin analog using palladium-catalyzed carbonylation trapping with *O*-enolate. *Heterocycles* **2017**, *94*, 1542−1553.
(35) Oettl, S. K.; Hubert, J.; Nuzillard, J.-M.; Stuppner, H.; Renault, J.-H.; Rollinger, J. M. Dereplication of depsides form the lichen *Pseudevernia furfuracea* by centrifugal partition chromatography combined to ^{13}C nuclear magnetic resonance pattern recognition. *Anal. Chim. Acta* **2014**, *846*, 60−67.
(36) Nomura, H.; Isshiki, Y.; Sakuda, K.; Sakuma, K.; Kondo, S. Effects of oakmoss and its components on biofilm formation of *Legionella pneumophila*. *Biol. Pharm. Bull.* **2013**, *36*, 833−837.
(37) Nomura, H.; Isshiki, Y.; Sakuda, K.; Sakuma, K.; Kondo, S. The antibacterial activity of compounds isolated from oakmoss against *Legionella pneumophila* and other *Legionella* spp. *Biol. Pharm. Bull.* **2012**, *35*, 1560−1567.
(38) Truong, B. N.; Pham, V. C.; Mai, H. D. T.; Nguyen, V. H.; Nguyen, M. C.; Nguyen, T. H.; Zhang, H.-J.; Fong, H. S. S.; Franzblau, S. G.; Soejarto, D. D.; Chau, V. M. Chemical constituents from *Xylosma longifolia* and their anti-tubercular activity. *Phytochem. Lett.* **2011**, *4*, 250−253.
(39) Li, Y.-R.; Li, G.-H.; Sun, L.; Li, L.; Liu, Y.; Kong, D.-G.; Wang, S.-Q.; Ren, D.-M.; Wang, X.-N.; Lou, H.-X.; Shen, T. Ingredients from *Litsea garrettii* as potential preventive agents against oxidative insult and inflammatory response. *Oxid. Med. Cell. Longevity* **2018**, *2018*, No. 7616852.
(40) Phetkul, U.; Phongpaichit, S.; Watanapokasin, R.; Mahabusarakam, W. New depside from *Citrus reticulata* Blanco. *Nat. Prod. Res.* **2014**, *28*, 945−951.
(41) Bissim, S. M.; kenmogne, S. B.; Tcho, A. T.; Lateef, M.; Ahmed, A.; Happi, E. N.; Wansi, J. D.; Ali, M. S.; Waffo, A. F. K. Bioactive acridone alkaloids and their derivatives from *Citrus aurantium* (Rutaceae). *Phytochem. Lett.* **2019**, *29*, 148−153.
(42) Salleh, W. M. N. H. W.; Ahmad, F. Phytochemistry and biological activities of the Genus *Knema* (Mysristicaceae). *Pharm. Sci.* **2017**, *23*, 249−255.
(43) Rukachaisirikul, V.; Naklue, W.; Sukpondma, Y.; Phongpaichit, S. An antibacterial biphenyl derivative from *Garcinia bancana* Miq. *Chem. Pharm. Bull.* **2005**, *53*, 342−343.
(44) Kihampa, C.; Nkunya, M. H. H.; Joseph, C. C.; Magesa, S. M.; Hassanali, A.; Heydenreich, M.; Kleinpeter, E. Anti-mosquito and antimicrobial *nor*-halimanoids, isocoumarins and an anilinoid from *Tessmannia densiflora*. *Phytochemistry* **2009**, *70*, 1233−1238.
(45) Mushtaq, M.; Alam, M. S.; Nahar, S.; Hashmi, M. H.; Ahmad, V. U. Secondary metabolites from a killer and antagonistic yeast strain, Y20-*Sporidiobolus ruineniae* and Y16-*Pichia anomala*. *Chem. Nat. Compd.* **2020**, *56*, 528−529.
(46) Lebeau, P.; Al-Hashimi, A.; Sood, S.; Lhoták, Š.; Yu, P.; Gyulay, G.; Peré, G.; Chen, S. R. W.; Trigatti, B.; Prat, A.; Siedah, N. G.; Austin, R. C. Endoplasmic reticulum stress and Ca^{2+} depletion differentially modulate the sterol regulatory protein PCSK9 to control lipid metabolism. *J. Biol. Chem.* **2017**, *292*, 1510−1523.
(47) Wu, Y.-R.; Li, L.; Sun, X.-C.; Wang, J.; Ma, C.-Y.; Zhang, Y.; Qu, H.-L.; Xu, R.-X.; Li, J.-J. Diallyl disulfide improves lipid metabolism by inhibiting PCSK9 expression and increasing LDL uptake via PI3K/Akt-SREBP2 pathway in HepG2 cells. *Nutr., Metab. Cardiovasc. Dis.* **2021**, *31*, 322−332.
(48) Lebeau, P. F.; Byun, J. H.; Platko, K.; Saliba, P.; Sguazzin, M.; MacDonald, M. E.; Paré, G.; Steinberg, G. R.; Janssen, L. J.; Igdoura, S. A.; Tarnopolsky, M. A.; Chen, S. R. W.; Seidah, N. G.; Magolan, J.; Austin, R. C. Caffeine blocks SREBP2-induced hepatic PCSK9 expression to enhance LDLR-mediated cholesterol clearance. *Nat. Commun.* **2022**, *13*, No. 770.
(49) Wang, J.; Wang, Y.-S.; Huang, Y.-P.; Jiang, C.-H.; Gao, M.; Zheng, X.; Yin, Z.-Q.; Zhang, J. Gypenoside LVI improves hepatic LDL uptake by decreasing PCSK9 and upregulating LDLR expression. *Phytomedicine* **2021**, *91*, No. 153688.
(50) Lin, Y.-K.; Yeh, C.-T.; Kuo, K.-T.; Yadav, V. K.; Fong, I.-H.; Kounis, N. G.; Hu, P.; Hung, M.-Y. Pterostilbene increase LDL metabolism in HL-1 cardiomyocytes by modulating the PCSK9/HNF1α/SREBP2/LDLR signaling cascade, upregulating epigenetic hsa-miR-335 and hsa-miR-6825, and LDL receptor expression. *Antioxidants* **2021**, *10*, 1280.
(51) Chae, H.-S.; Kim, H. J.; Ko, H.-J.; Lee, C. H.; Choi, Y. H.; Chin, Y.-W. Transcriptome analysis illuminates a hub role of *SREBP2*

https://doi.org/10.1021/acsomega.2c06660
ACS Omega 2022, 7, 47296−47305

in cholesterol metabolism by α-mangostin. *ACS Omega* **2020**, *5*, 31126−31136.
(52) Chen, S.-F.; Chen, P.-Y.; Hsu, H.-J.; Wu, M.-J.; Yen, J.-H. Xanthohumol suppresses mylip/idol gene expression and modulates LDLR abundance and activity in HepG2 cells. *J. Agric. Food Chem.* **2017**, *65*, 7908−7918.
(53) Zhang, L.; Fairall, L.; Goult, B. T.; Calkin, C. H.; Hong, C.; Millard, C. J.; Tontonoz, P.; Schwabe, J. W. R. The IDOL-UBE2D complex mediates sterol-dependent degradation of the LDL receptor. *Genes Dev.* **2011**, *25*, 1262−1274.
(54) Leitch, E. K.; Elumalai, N.; Fridén-Saxin, M.; Dahl, G.; Wan, P.; Clarkson, P.; Valeur, E.; Pairaudeau, G.; Boyd, H.; Tavassoli, A. Inhibition of low-density lipoprotein receptor degradation with a cyclic peptide that disrupts the homodimerization of IDOL E3 ubiquitin ligase. *Chem. Sci.* **2018**, *9*, 5957−5966.
(55) Adasme, M. F.; Linnemann, K. L.; Bolz, S. N.; Kaiser, F.; Salentin, S.; Haupt, V. J.; Schroeder, M. PLIP 2021: expanding the scope of the protein-ligand interaction profiler to DNA and RNA. *Nucleic Acids Res.* **2021**, *49*, W530−W534.

https://doi.org/10.1021/acsomega.2c06660
ACS Omega 2022, 7, 47296−47305